JGR Planets

RESEARCH ARTICLE
10.1029/2019JE006156

Reevaluation of Perchlorate in Gale Crater Rocks Suggests Geologically Recent Perchlorate Addition

Peter E. Martin[1], Kenneth A. Farley[1], P. Douglas Archer Jr[2], Joanna V. Hogancamp[2], Kirsten L. Siebach[3], John P. Grotzinger[1], and Scott M. McLennan[4]

[1]Division of Geological and Planetary Sciences, California Institute of Technology, Pasadena, CA, USA, [2]Jacobs, NASA Johnson Space Center, Houston, TX, USA, [3]Earth, Environmental, and Planetary Sciences, Rice University, Houston, TX, USA, [4]Department of Geosciences, Stony Brook University, Stony Brook, NY, USA

Key Points:
- Geology suggests that ancient Gale crater was not conducive to perchlorate deposition; radiolytic decomposition would destroy ancient perchlorate
- Alternatives to perchlorate are evaluated as sources of pyrolytic O_2; perchlorate best explains the data
- Perchlorate in Gale crater is most likely young, possibly introduced by downward percolation of thin films of brine

Supporting Information:
- Supporting Information S1

Correspondence to:
P. E. Martin,
pmmartin@caltech.edu

Citation:
Martin, P. E., Farley, K. A., Douglas, P., Jr, Hogancamp, J. V., Siebach, K. L., Grotzinger, J. P., & McLennan, S. M. (2020). Reevaluation of perchlorate in Gale crater rocks suggests geologically recent perchlorate addition. *Journal of Geophysical Research: Planets*, *125*, e2019JE006156. https://doi.org/10.1029/2019JE006156

Received 7 AUG 2019
Accepted 16 JAN 2020
Accepted article online 30 JAN 2020

Abstract Perchlorate (ClO_4^-) was discovered in Martian soil by the Phoenix lander, with important implications for potential Martian biology, photochemistry, aqueous chemistry, and the chlorine cycle on Mars. Perchlorate was subsequently reported in both loose sediment and bedrock samples analyzed by the Sample Analysis at Mars instrument onboard the Curiosity rover in Gale crater based on a release of O_2 at 200–500°C. However, the continually wet paleoenvironment recorded by the sedimentary rocks in Gale crater was not conducive to the deposition of highly soluble salts. Furthermore, the preservation of ancient perchlorate to the modern day is unexpected due to its low thermodynamic stability and radiolytic decomposition associated with its long exposure to radioactivity and cosmic radiation. We therefore investigate alternative sources of O_2 in Sample Analysis at Mars analyses including superoxides, sulfates, nitrate, and nanophase iron and manganese oxides. Geochemical evidence and oxygen release patterns observed by Curiosity are inconsistent with each of these alternatives. We conclude that perchlorate is indeed the most likely source of the detected O_2 release at 200–500°C, but contend that it is unlikely to be ancient. Rather than being associated with the lacustrine or early diagenetic environment, the most likely origin of perchlorate in the bedrock is late stage addition by downward percolation of water through rock pore space during transient wetting events in the Amazonian. The conclusion that the observed perchlorate in Gale crater is most likely Amazonian suggests the presence of recent liquid water at the modern surface.

Plain Language Summary Perchlorate is a chemical found on Mars that dissolves easily in water, which can keep water from freezing at the cold temperatures found on Mars's surface. It was first discovered in soil, and has been found by the Curiosity rover in rock at Gale crater. Perchlorate should have flowed out of the sandy lake bottom in ancient Gale crater before it turned into rock. Perchlorate is also easily destroyed, so even if it were included in the rock originally, perchlorate should have disintegrated in the following ~3.5 billion years. Because of these dilemmas with finding perchlorate in ancient rocks, we have reevaluated the evidence for perchlorate as observed by Curiosity. Of a number of other chemicals which could explain the data, we find that perchlorate is still the best fit and is probably present. Due to the problems with perchlorate being included in the rock originally and surviving until today, we conclude that it has been added to the rocks recently. This recent addition could happen by perchlorate dissolving in water and flowing into the rock. Such a process suggests that liquid water was present in Gale crater long after Mars became cold and dry.

1. Introduction

Perchlorate anion (ClO_4^-) was discovered in Martian soil in 2009 by the Phoenix Lander (Hecht et al., 2009), spurring discussion of the implications for potential Martian biology, photochemistry, aqueous chemistry, and the chlorine cycle on Mars. Central to perchlorate's importance is its exceptional solubility, which allows freezing point depression in saturated fluids of up to −75°C (Marion et al., 2010; Toner et al., 2014, 2015). Perchlorate salts are also highly hygroscopic, deliquescing at the low temperatures and relative humidities of 243 K and <40%, respectively (Gough et al., 2014). These combined traits allow the spontaneous formation of liquid perchlorate brines, even at Mars surface conditions. As a result, perchlorate has been invoked to explain observations such as recurring slope lineae (e.g., Chevrier & Rivera-Valentin, 2012; McEwen et al., 2011) and putative sub-polar cap liquid water (Orosei et al., 2018). Perchlorate may act as an electron acceptor for microbes (McKay et al., 2013; Oren et al., 2014), and may destroy organic molecules via

interaction with intermediate oxidation steps during perchlorate formation (Carrier & Kounaves, 2015), interaction with ionizing radiation (Quinn et al., 2013), or during analytical heating of a sample (Lasne et al., 2016; ten Kate, 2010), impacting the search for potential biosignatures.

The discovery of perchlorate by Phoenix was compellingly made using three lines of evidence: (1) an ion-selective electrode with a high perchlorate sensitivity indicated the presence of perchlorate; (2) an electrode designed for Ca^{2+} measurement fell, consistent with a known interference from perchlorate; and (3) a release of oxygen was detected during heating of soil samples, interpreted as a result of perchlorate breakdown (Hecht et al., 2009).

The Tissint Mars meteorite has been observed to contain ppb levels of perchlorate along with other oxychlorine phases, which are likely Martian in origin (Jaramillo et al., 2019). Additional detections of perchlorate on Mars have been equivocal. The Shergottite EETA79001 contains perchlorate and nitrate, which isotopically contrasts with the surrounding ice and rock, but matches the isotopic composition of nitrate in the Atacama (Kounaves et al., 2014), leaving its origin ambiguous. The putative in situ detection of perchlorate based on orbital spectroscopy (Ojha et al., 2015) was shown to be the result of a spectral artifact (Leask et al., 2018). Viking data were reinterpreted as consistent with perchlorate based on the presence of chloromethane (Navarro-González et al., 2010), although this interpretation has been challenged (Biemann & Bada, 2011).

The first evolved gas analysis (EGA) of a scooped soil sample by the Sample Analysis at Mars (SAM) instrument on the Curiosity rover yielded temporally correlated detections of O_2 and chlorinated hydrocarbons, interpreted as evidence of an oxychlorine phase such as perchlorate in the soil at Gale crater (Glavin et al., 2013; Leshin et al., 2013). Later analysis of a sample of ancient lacustrine bedrock produced similar results (Ming et al., 2014). Perchlorate has since been suggested to be present in additional samples of ancient Gale crater rocks (Sutter et al., 2017) as an original component of those samples (Archer et al., 2016). We use the term "indigenous perchlorate" to refer to putative perchlorate deposited as a lacustrine material in the Gale crater lake or by early diagenetic fluids. We refer to perchlorate rather than oxychlorine or (per)chlorate (as chlorate may explain these observations; Hogancamp, Archer, et al., 2018; Sutter et al., 2017); the arguments throughout apply to both chlorate and perchlorate with the caveat that chlorate is far less kinetically stable (section 2.1.2).

Another line of evidence supporting perchlorate in Gale crater is the presence of highly unusual chlorine isotope compositions. While the vast bulk of chlorine reservoirs on Earth vary within ±3‰ $\delta^{37}Cl$ (Eggenkamp, 2014), chlorine isotope ratios in Gale crater measured on HCl are strongly depleted in ^{37}Cl and highly variable: −50 to −15‰ $\delta^{37}Cl$ (Farley et al., 2016). Either direct measurement of oxychlorine phases or cycling of chlorine through oxychlorine phases was the preferred interpretation of Farley et al. (2016). This interpretation was based heavily on analogy with the findings of extremely isotopically ^{37}Cl-depleted perchlorate in the Atacama, fractionated via an unknown mechanism (Böhlke et al., 2005).

The presence of indigenous perchlorate would have significant implications for early Mars and thus warrants critical appraisal. We present evidence that the depositional and early diagenetic paleoenvironments of the bedrock in Gale crater were not conducive to perchlorate deposition/preservation, and that perchlorate deposited at that time is expected to have decomposed in the billions of years after deposition. We therefore consider two alternative explanations to indigenous perchlorate for the oxygen release observed in samples from Gale crater: the oxygen is produced by a substance other than perchlorate, or it is produced by perchlorate that is not indigenous. Our assessment shows that perchlorate remains the most consistent explanation for SAM EGA observations, and that the simplest solution to the paradox of perchlorate in the ancient sedimentary rocks in Gale crater is that the perchlorate was introduced long after rock deposition. We hypothesize that it has been introduced by percolation of water into the pore spaces of the bedrock in Gale crater during infrequent wetting events.

2. Perchlorate in Gale Crater

In this section we describe challenges to the deposition of perchlorate during bedrock formation in Gale crater and its subsequent preservation. We then consider the evidence offered in support of perchlorate as measured by the SAM instrument. We show that the presence of a large release of O_2 at 200–500°C is the only

line of evidence that cannot be explained by compounds independently confirmed to be present by other instruments.

2.1. Evidence Against Ancient Perchlorate Based on Geologic Interpretation

2.1.1. Geologic Evidence

The geologic setting of bedrock deposition in Gale crater was not likely conducive to perchlorate precipitation. The stratigraphy observed in Gale crater includes mostly fluvial and deltaic sandstones and lacustrine mudstones, the latter of which indicate fresh to mildly saline lake waters (e.g., Grotzinger et al., 2015, 2014; Stack et al., 2019). This setting differs from where perchlorate salts are found on Earth, in arid environments such as the Antarctic Dry Valleys and the Atacama (Ericksen, 1981; Kounaves et al., 2010). Perchlorate salts form via extremely concentrated brines, and are highly vulnerable to dissolution and consequently unlikely to be incorporated into the rock record. On Earth, the perchlorate ion is only ever found as a minor ($\leq$0.1 wt %) constituent in soils, caliches, and surficial evaporites (Jackson et al., 2015). In order to be included in the rock record, a perchlorate deposit would need to precipitate as a salt from solution, and subsequently have extremely limited open-system interactions with liquid water during and after lithification (and avoid reduction via biotic interactions; Coates & Achenbach, 2004). Such a scenario is conceivable on Mars, but the rocks so far explored in Gale crater are conformable lacustrine deposits that document a continually wet environment, rather than evaporite beds (Grotzinger et al., 2015).

Other less soluble salt species such as Ca-, Mg-, and Fe-sulfate and various chloride salts (e.g., Hardie et al., 1978; Tosca et al., 2005) would be expected at high abundance in the bulk rock in concert with the perchlorate salts or in discrete highly concentrated layers if more soluble ions were ever precipitated. Calcium sulfate minerals are common, but in late fractures that cross-cut bedding as well as major unconformities (Caswell & Milliken, 2017; Grotzinger et al., 2014; Vaniman et al., 2014, 2018). Abundant bedded evaporite deposits have not been observed, although small amounts of highly soluble Fe- and $MgSO_4$ (Sutter et al., 2017) and chloride salts (Thomas et al., 2018) have been observed in the rock matrix. The possibility therefore exists that other highly soluble salts (including perchlorate) were also included via an unknown mechanism.

Common indicators of aridity such as convolute bedding, enterolithic folding, tepee structures, and displacive/massive evaporite mineral growth are not observed. In only one location have desiccation cracks been confidently observed (Stein et al., 2018). On the other hand, numerous indications of later diagenetic processes extending as much as ~1.5 Ga after the original deposition of the lacustrine rocks have been noted (e.g., Grotzinger et al., 2015; Martin, Farley, Baker, et al., 2017; Nachon et al., 2014), lengthening the timeline of aqueous interaction within this rock sequence. If any perchlorate had precipitated in the early environment, these later fluids could have dissolved and removed it. This idea was suggested by Archer et al. (2016) based on the smaller amount of O_2 released from the vein-rich sample John Klein relative to the nearby, more pristine Cumberland sample. This contrast between Cumberland and John Klein also suggests that a late addition of perchlorate by diagenetic fluids is unlikely (Archer et al., 2016).

2.1.2. Thermodynamics and Radiolysis

The thermodynamic instability of perchlorate lowers the likelihood of its long-term survival in Martian bedrock. While perchlorate ion has a high thermodynamic oxidative potential (Urbansky, 2002), it is kinetically stable, impeding reduction in most settings (Brown & Gu, 2006). However, decomposition of perchlorate occurs under exposure to ionizing radiation (Prince & Johnson, 1965a; Quinn et al., 2013; Turner et al., 2016). While UV interactions have been proposed as a formation mechanism for perchlorate (e.g., Carrier & Kounaves, 2015; Wilson et al., 2016), this thermodynamically unfavorable process occurs only when a local energy minimum is encountered. The radiolysis breakdown described above allows the kinetic barrier to be broken so that thermodynamically favorable decomposition can occur. This decomposition results in the formation of chlorate (ClO_3^-), chlorite (ClO_2^-), chlorine dioxide (ClO_2), hypochlorite (ClO^-), and chloride (Cl^-), although the final product of decomposition is most likely chloride (see the discussion of chlorate below; Prince & Johnson, 1965a). Martian rocks are exposed to ionizing radiation from the radioactive decay of ^{40}K and U- and Th-series isotopes, and from galactic cosmic rays (GCRs) in the uppermost few meters of the surface.

The dose of ionizing radiation from radioactive decay experienced by a rock can be computed from the depositional age of the rock and its radioelement content. On Curiosity, K is measured by both ChemCam and APXS. Although no instruments currently deployed on the surface of Mars can measure U or Th,

Table 1
Radiolysis Calculations for Each Sample

Sample	K_2O (wt %)	Radiogenic dose (MGy)	Measured exposure age (Ma)	Min|Max GCR (MGy)		Min|Max total (MGy)		Min|Max % destroyed	
OG	0.59 ± 0.07	**13.6 ± 1.8**	-	4.4 ± 1.9	69.4 ± 18.6	18.0 ± 2.6	83.1 ± 18.7	60.0 ± 9.2	98.6 ± 22.7
GB1	0.49 ± 0.06	**11.3 ± 1.5**	-	4.4 ± 1.9	69.4 ± 18.6	15.7 ± 2.4	80.7 ± 18.6	55.1 ± 8.9	98.4 ± 23.2
GB2	0.40 ± 0.05	**9.2 ± 1.2**	-	4.4 ± 1.9	69.4 ± 18.6	13.6 ± 2.3	78.7 ± 18.6	50.0 ± 8.7	98.2 ± 23.7
RN	1.86 ± 0.22	**42.9 ± 5.7**	-	4.4 ± 1.9	69.4 ± 18.6	47.3 ± 6.0	112.3 ± 19.4	91.0 ± 12.4	99.7 ± 18.0
RH	0.58 ± 0.07	**13.4 ± 1.8**	-	4.4 ± 1.9	69.4 ± 18.6	17.7 ± 2.6	82.8 ± 18.7	59.6 ± 9.1	98.5 ± 22.7
HF	0.9 ± 0.11	**20.8 ± 2.7**	-	4.4 ± 1.9	69.4 ± 18.6	25.1 ± 3.3	90.2 ± 18.8	72.3 ± 10.2	99.0 ± 21.2
ST	0.91 ± 0.11	**21.0 ± 2.8**	-	4.4 ± 1.9	69.4 ± 18.6	25.4 ± 3.4	90.4 ± 18.8	72.6 ± 10.3	99.0 ± 21.1
DU	0.94 ± 0.11	**21.7 ± 2.9**	-	4.4 ± 1.9	69.4 ± 18.6	26.0 ± 3.3	91.1 ± 18.8	73.5 ± 10.4	99.0 ± 21.0
QL	0.77 ± 0.09	**17.8 ± 2.3**	-	4.4 ± 1.9	69.4 ± 18.6	22.1 ± 3.0	87.2 ± 18.7	67.7 ± 9.8	98.8 ± 21.8
MB	0.83 ± 0.10	**19.1 ± 2.5**	-	4.4 ± 1.9	69.4 ± 18.6	23.5 ± 3.2	88.6 ± 18.7	69.9 ± 10.0	98.9 ± 21.5
BY	0.49 ± 0.06	**11.3 ± 1.5**	-	4.4 ± 1.9	69.4 ± 18.6	15.7 ± 2.4	80.7 ± 18.6	55.1 ± 8.9	98.4 ± 23.2
GH	0.29 ± 0.03	**6.7 ± 0.9**	-	4.4 ± 1.9	69.4 ± 18.6	11.1 ± 2.1	76.1 ± 18.6	43.1 ± 8.4	98.0 ± 24.4
OU	0.81 ± 0.10	**18.7 ± 2.5**	-	4.4 ± 1.9	69.4 ± 18.6	23.1 ± 3.1	88.1 ± 18.7	69.2 ± 9.9	98.9 ± 21.6
BK	1.00 ± 0.12	**23.0 ± 3.0**	-	4.4 ± 1.9	69.4 ± 18.6	27.4 ± 3.6	92.5 ± 18.8	75.3 ± 10.5	99.1 ± 20.8
TP	0.98 ± 0.12	**22.6 ± 3.0**	-	4.4 ± 1.9	69.4 ± 18.6	27.0 ± 3.5	92.0 ± 18.8	74.8 ± 10.5	99.1 ± 20.8
MJ	0.63 ± 0.08	**14.5 ± 1.9**	**1240 ± 220**	**69.4 ± 18.6**		**84.0 ± 18.7**		**98.6 ± 22.5**	
CH	0.98 ± 0.12	**22.6 ± 3.0**	-	4.4 ± 1.9	69.4 ± 18.6	27.0 ± 3.5	92.0 ± 18.8	74.8 ± 10.5	99.0 ± 20.8
WJ	3.09 ± 0.37	**71.3 ± 9.4**	**55 ± 43**	**3.1 ± 2.5**		**74.3 ± 9.7**		**97.8 ± 13.7**	
JK	0.54 ± 0.06	**12.5 ± 1.6**	-	4.4 ± 1.9	69.4 ± 18.6	16.8 ± 2.5	81.9 ± 18.6	57.6 ± 9.1	98.5 ± 22.9
CB	0.62 ± 0.07	**14.3 ± 1.9**	**78 ± 30**	**4.4 ± 1.9**		**18.7 ± 2.7**		**61.4 ± 9.3**	

Note. Bold numbers indicate that no extrapolation from other samples has been performed. Radiogenic dose is inferred from K_2O measurements, and exposure ages are directly measured. Samples are shown in stratigraphic order (lowest = lowest in the section). Rows shaded in blue are scooped sediment samples. Rows shaded in red do not have a measured O_2 release. All uncertainties are at the 1-σ level. GCR = "galactic cosmic ray," CB = Cumberland, JK = John Klein, WJ = Windjana, CH = Confidence Hills, MJ = Mojave, TP = Telegraph Peak, BK = Buckskin, OU = Oudam, GH = Greenhorn, BY = Big Sky, MB = Marimba, QL = Quela, DU = Duluth, ST = Stoer, HF = Highfield, RH = Rock Hall, OG = Ogunquit Beach, GB = Gobabeb, RN = Rocknest.

these three elements do not greatly fractionate from one another in igneous processes. Based on orbital gamma ray spectral mapping of K and Th abundances in the near surface, the best estimate for the average Martian K/Th ratio is 5,330 (Taylor et al., 2007), which is also consistent with Martian meteorite data that further indicate a K/U ratio of about 20,000 (e.g., Taylor, 2013; Taylor & McLennan, 2009; Wänke et al., 1994). Using measurements of K_2O content (Bristow et al., 2018; Morrison et al., 2018), these assumed elemental ratios, the isotopic heat production values from Van Schmus (1995), and a depositional age of 3.6 Ga (Le Deit et al., 2012), we calculate that the total accumulated radiogenic radiation dose of the samples analyzed by SAM ranges from 6.7 ± 0.9 to 71.3 ± 9.4 MGy (all uncertainties at the 1-σ level, see section S2 for detailed description of uncertainty derivation and Table 1).

The exposure of Gale crater rocks to radiation from GCRs is less well known, but can be estimated from reported cosmic ray exposure ages (Farley et al., 2014; Martin, Farley, Mahaffy, et al., 2017; Vasconcelos et al., 2016) and modeled GCR dose rates (Pavlov et al., 2012). For samples with no measured exposure age, we take the well-constrained exposure ages measured at Cumberland and Mojave 2 as lower and upper bounds of GCR radiation dose. Table 1 shows the results of these calculations, and demonstrates that the average minimum total dose of ionizing radiation experienced at the surface in Gale crater is ~30 MGy, mostly coming from radioactive decay rather than from GCRs.

Given these ionizing radiation doses, the fraction of indigenous 3.6 Ga perchlorate destroyed since deposition may be calculated (Table 1). We adopt the radiolysis rates reported by Prince and Johnson (1965a) for $KClO_4$ as this yields the lowest breakdown rate and thus provides a conservative estimate of perchlorate radiolysis. Prince and Johnson (1965a, 1965b) studied the destruction of the perchlorate ion and the ingrowth of breakdown products for multiple perchlorate salts with carefully monitored dose rates and at a sufficiently high radiation dose (~5 MGy) that the radiolytic decomposition rate was well defined. Other studies investigated the products of radiolytic perchlorate decomposition but did not report perchlorate radiolysis constants (Quinn et al., 2013; Turner et al., 2016). For these studies we computed radiolysis constants from

reported results and found that they agree with the precise estimates of Prince and Johnson (1965a) to within about a factor of 2. Radiolysis is essentially independent of temperature, pressure, and cation of the perchlorate salt (Prince & Johnson, 1965b), suggesting that laboratory rates are applicable to the Martian surface throughout Martian history. However, as no study has evaluated perchlorate radiolysis on a geologically relevant matrix, further experiments could be undertaken to refine radiolysis constants for perchlorate.

For some of the analyzed rocks the estimated fraction of surviving putative indigenous perchlorate is prohibitive. The sample Windjana is the most potassic yet analyzed by SAM, providing an end-member for the radiogenic component of the ionizing radiation dose. The radiation dose for Windjana is 74.3 ± 9.7 MGy, which would destroy 97.8 ± 13.7% of any indigenous perchlorate (Table 1). Given Windjana's perchlorate content of 0.23 ± 0.06 wt %, the original perchlorate content would have to have been 10.2 ± 3.0 wt %, 2 orders of magnitude higher than the maximum concentration observed on Earth (Jackson et al., 2015) and ~20 times that inferred at the Phoenix landing site (Hecht et al., 2009). Additionally, if nearly 10 wt % of the original rock were destroyed, collapse structures and/or void space would be expected, but are not observed. This conclusion is further strengthened by considering the Cl budget of the rock. Given Windjana's APXS-measured Cl content of 0.57 ± 0.09 wt % and its putative perchlorate content of 0.23 ± 0.06 wt % (0.082 ± 0.02 wt % as Cl)(Sutter et al., 2017), 14.4 ± 4.3% of the total Cl in Windjana is presently in the form of perchlorate. If 97.8 ± 13.7% of indigenous perchlorate has decomposed to chloride, then at most 2.3 ± 0.3% of the chlorine in Windjana could be in the form of perchlorate if all chlorine in the sample was originally perchlorate, clearly inconsistent with the current amount of perchlorate.

These calculations may not be prohibitive if perchlorate is reduced only to chlorate rather than to chloride. SAM data cannot distinguish among oxychlorine compounds, so either chlorate or perchlorate could explain the SAM data (Hogancamp, Archer, et al., 2018). Chlorate is thermodynamically unstable (e.g., Brown & Gu, 2006; Srinivasan et al., 2009), likely suffering the same radiolysis fate as perchlorate. Chlorate is an initial product of perchlorate decomposition in radiolysis experiments (Prince & Johnson, 1965a; Turner et al., 2016), but it is not necessarily the stable end product of radiolysis. Unlike perchlorate, chlorate is kinetically unstable (e.g., Brown, 1986; Cao et al., 2005; Gu et al., 2003) and is reduced to chloride by Fe^{2+} on a time scale of hours to days (Gu et al., 2003; Mitra & Catalano, in press), suggesting that it may not survive long enough to be destroyed by radiation due to (electro)chemical reduction. It appears most likely that chlorate reduction quickly follows radiolysis and perchlorate is rapidly reduced to Cl^- in a stepwise fashion, as observed in numerous instances on Earth (e.g., Cao et al., 2005; Gu et al., 2003; Urbansky, 2002). Thus, indigenous chlorate no better accounts for these observations than perchlorate.

2.2. Putative Perchlorate Detection by SAM

No corroborating evidence for the presence of perchlorate has been obtained from any other instrument on Curiosity (e.g., ChemCam or CheMin; Gasnault et al., 2012), which is expected because, even at the highest reported levels, the perchlorate is at or below the detection limits of these instruments. In light of the geologic observations that make deposition and survival of perchlorate in ancient Gale crater rocks highly unlikely, and in the absence of corroborating data, it is important to reexamine the varied lines of evidence from SAM that have been offered in favor of its presence.

Rock and regolith samples are delivered to SAM after scooping sediment from the surface or drilling to collect bedrock 1.5–5 cm below the surface (Anderson et al., 2012). A mass of sample between 45 ± 6 and 135 ± 18 mg is gradually heated to ~900°C, releasing volatile species (e.g., Sutter et al., 2017). A helium stream acts as a carrier gas, sweeping evolved volatiles into a quadrupole mass spectrometer (Mahaffy et al., 2012), allowing temperature-resolved EGA. For rare isotopologues or uncommon gas species, careful correction for isobaric interferences must be made (e.g., Archer et al., 2014; Eigenbrode et al., 2018; Sutter et al., 2017). However, the gases analyzed here are sufficiently abundant that the raw signal of m/z corrected only for detector deadtime is used as a proxy for the gas of interest (i.e., $O_2 = m/z$ 32; HCl = m/z 36).

The first SAM EGA run on a solid sample was a scooped sand shadow deposit called Rocknest. A large release of O_2 (m/z 32) was observed with chloromethane (CH_3Cl, m/z 50 and 52) released at the onset of O_2 evolution (Figure S1; Leshin et al., 2013), interpreted as evidence for perchlorate (Glavin et al., 2013; Leshin et al., 2013). A similar correlation was noted in the first drilled bedrock samples, although a temporal

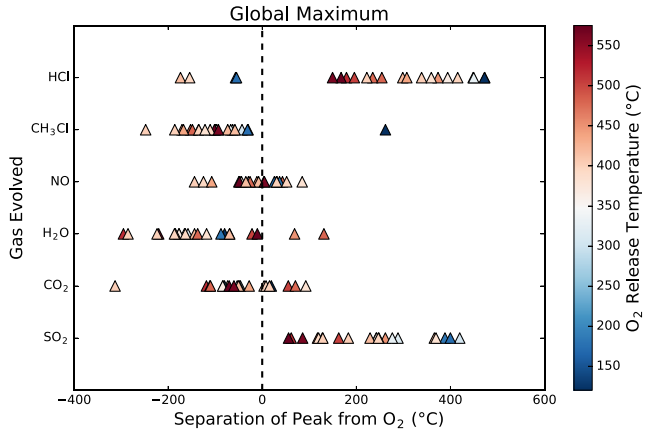

Figure 1. The global maximum gas release temperatures for a variety of gases relative to the maximum gas release temperature of O_2. The color bar shows the absolute temperature of maximum O_2 release. No strong correlation exists between the release temperature of O_2 and HCl and CH_3Cl. However, NO is released near or simultaneously to O_2, regardless of the absolute temperature of O_2 release.

connection with HCl (*m*/*z* 36 and 38) was invoked as well (Ming et al., 2014). Samples collected later in the mission also produced large O_2 releases attributed to perchlorate (Sutter et al., 2017).

Figure 1 shows that the temporal correlations among O_2, HCl, and CH_3Cl are not especially strong relative to other abundant gases released during EGA with no known association to perchlorate. This conclusion holds regardless of exactly how the timing is established (e.g., initial onset of release, peak release, or any combination of these; Figure S2). Similarly, the detailed temporal relationships among O_2, HCl, and chloromethane are inconsistent among samples (Figure S1).

This lack of temporal correlation between HCl and O_2 is not surprising. While Fe- and Mg- perchlorate salts are thought to release HCl and O_2 simultaneously, for other cations perchlorate breakdown proceeds by release of O_2 and formation of chloride salts which then release HCl only when sufficient water is available for protonation (Hogancamp et al., 2017; Sutter et al., 2017). This decoupling between HCl and perchlorate-generated O_2 means that it is impossible to know whether HCl is a product of perchlorate breakdown or was released from chloride salts originally in the sample. If an alternative source of O_2 is present, no perchlorate is required by these observations and all HCl detected by SAM could be sourced from chloride (Hogancamp et al., 2017; Sutter et al., 2017). On the other hand, since a temporal correlation between O_2 and HCl is not expected in the decomposition of all perchlorate salts, the absence of such a correlation is not evidence against the presence of perchlorate.

In many samples, the main release of CH_3Cl occurs as the release of O_2 is beginning (Figure S2d; Glavin et al., 2013; Leshin et al., 2013). This ordering is likely not evidence for perchlorate in the sample; its tetrahedral structure presumably prevents interaction of organics with the central chlorine atom until *after* the perchlorate anion has broken down and released O_2. Furthermore, chlorinated hydrocarbons have been produced via heating of chloride salts (Keppler et al., 2014), signifying that the chlorinated hydrocarbons in EGA could be explained by either perchlorate or chloride salts.

Independent of release temperature correlations, consistent molar ratios between O_2 and CH_3Cl or HCl might indicate the presence of perchlorate. No such correlation is evident however (Figure 2). Numerous and complex reactions likely occur between the gases released during EGA, between these gases and the rock sample, and potentially within the SAM transfer lines. A lack of correlation in measured abundance therefore does not preclude a correlation in abundance of gases released from the sample, but there is no evidence to support the presence of perchlorate based on measured abundances.

In the samples Oudam, Marimba, Quela, Duluth, and Stoer, no evolved O_2 was detected (Table 1 and Figure S1), an observation attributed to the absence of >0.06 wt % perchlorate (the estimated detection limit) in these rocks (Archer et al., 2019). These samples were not included in the temporal correlation assessments described above to avoid potential sampling bias against perchlorate. However, the release patterns of HCl and CH_3Cl in these runs are indistinguishable from the patterns observed in O_2-bearing samples (Figure S1), and in fact, *more* HCl and CH_3Cl are present (Figure 2). These observations compellingly argue that the HCl and CH_3Cl peaks in EGA runs are agnostic as to whether perchlorate is present.

2.3. Is Perchlorate Present in Modern Gale Crater Sediment Deposits?

The above discussion centers on the improbability of finding perchlorate indigenous to the ancient sedimentary rocks found in Gale crater. By analogy to the Phoenix perchlorate detection in modern Martian soil (Hecht et al., 2009), perchlorate may have been deposited on and mixed into modern eolian materials in Gale crater. The assessments performed in section 2.2 were repeated using only scooped sediment/regolith samples (Figure S3); in these modern eolian samples there is no correlation between O_2 and HCl or CH_3Cl. As the drilled bedrock samples and scooped samples are not distinguishable in these analyses, there are two straightforward possibilities: either perchlorate is present in both, evidenced only by the release of O_2,

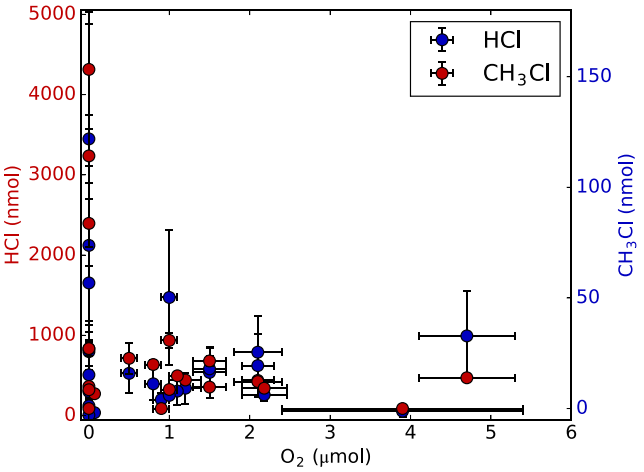

Figure 2. The molar amount of HCl and CH_3Cl measured in each sample plotted against the amount of O_2 observed. No correlation between these gases is observed.

or perchlorate is not present in either sample set and another compound is responsible for the observed O_2 release.

There is also no apparent enrichment in O_2 release in these samples (Figure S3), suggesting that perchlorate is no more abundant in surface materials than near-surface materials. The perchlorate formation mechanism on Mars is debated and may involve irradiation of the surface (Carrier & Kounaves, 2015; Wilson et al., 2016; Zhao et al., 2018), atmospheric interactions (Catling et al., 2010; Smith et al., 2014), or electrochemical processes (Steele et al., 2018). Each of these mechanisms would likely result in enrichment of perchlorate at the surface. This lack of additional O_2 in these surface samples relative to drilled bedrock suggests that perchlorate is not enriched in surface materials relative to the shallow subsurface of the rock (1.5–5-cm depth), which may indicate perchlorate equilibration between these locations (discussed further in section 4).

3. Alternative Explanations for O_2 Release

The only SAM observation attributed to perchlorate that cannot be explained exclusively by the presence of chloride salts is a large release of O_2 between 200 and 500°C. Several chemical species (including perchlorate) could be responsible for this oxygen release. Rather than suggest ad hoc explanations for the observed low- to moderate-temperature O_2 release in each sample, we propose that a single chemical species is likely the major source of this O_2 in every sample. Here we attempt to present a comprehensive list of potential O_2 sources and discuss the viability of each as candidate sources of the SAM-observed O_2.

3.1. Hydrogen Peroxide/Superoxides

Superoxides (including hydrogen peroxide) were invoked to explain the release of O_2 and the lack of detected organics by the Viking mission (Oyama & Berdahl, 1977). Modeling and observation suggest that hydrogen peroxide exists in the Martian atmosphere and likely at the surface (Atreya et al., 2006; Atreya & Gu, 1994; Encrenaz et al., 2004). However, these species are temperature-stable only up to ~200°C (Yen et al., 2000; Zent et al., 2008). O_2 releases in SAM extend well above this temperature, so peroxides and superoxides can be ruled out.

3.2. Sulfates

Sulfates release O_2 upon heating (Gallagher et al., 1970; Holt & Engelkemeir, 1970), and are present in high abundance in veins permeating Gale crater (e.g., Nachon et al., 2014; Rampe et al., 2017). However, the release of O_2 from sulfate is always coincident with that of SO_2, which is not observed in the O_2 releases between 200 and 500°C attributed to perchlorate (Sutter et al., 2017). Such a correlation is observed in the higher temperature 500–700°C O_2 releases, which are thought to result from the breakdown of Fe- and/or Mg-sulfate (Sutter et al., 2017). Sulfates can therefore be eliminated as the source of the 200–500°C O_2 in SAM.

3.3. Nitrate

The release of NO in EGAs has been attributed to the breakdown of nitrate in SAM (Stern et al., 2015). The NO/O_2 molar ratio is consistent among EGA samples, which has been interpreted as evidence for a constant nitrate/perchlorate ratio and a related formation mechanism (Stern et al., 2017). Not only does NO correlate with O_2 by molar amount, but the NO release is correlated in time with the O_2 releases in nearly all samples, regardless of the absolute temperature of O_2 release (Figures 1 and S2). This double correlation raises the possibility that nitrate breakdown is the major source of O_2 in the samples. While nitrate breakdown does produce both NO and O_2 gases, the NO/O_2 ratio in EGA is ~1:20 (Stern et al., 2017), far lower than the expected 1:1 ratio for nitrate breakdown. We therefore rule out nitrate as a major contributor to the O_2 signal observed by SAM, as did Sutter et al. (2017).

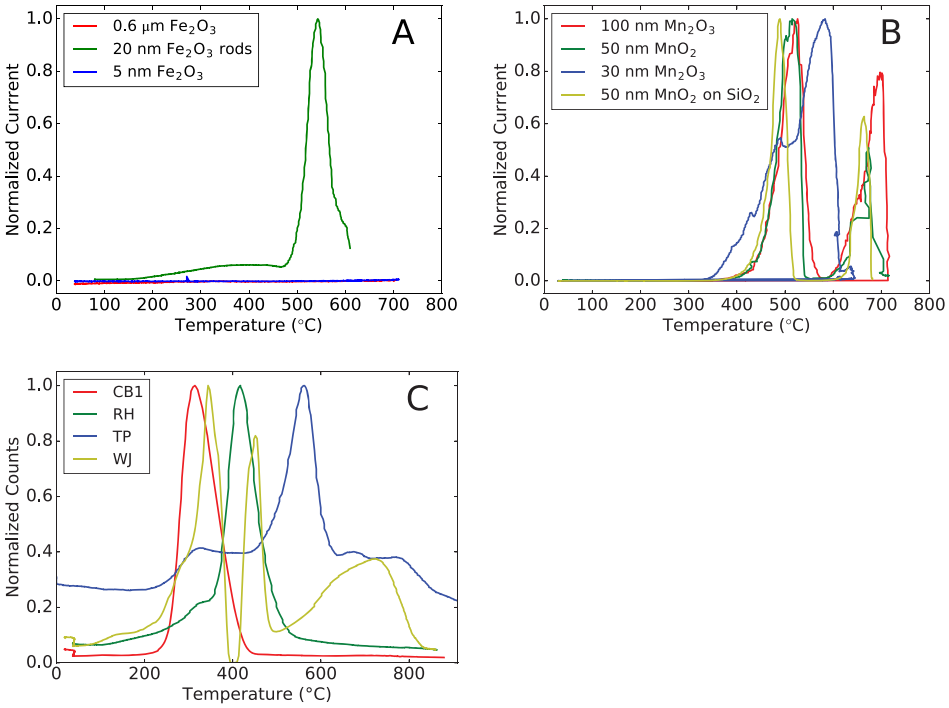

Figure 3. (a) Iron oxide-sourced O_2 gas traces. (b) Manganese oxide-sourced O_2 gas traces. (c) Example O_2 (m/z 32) traces from samples throughout the Curiosity mission, smoothed with a 10-point running mean. All gas traces normalized to a maximum value of 1.

3.4. Metal Oxides

Metal oxides and oxyhydroxides are also a candidate source of the SAM O_2 peak. When heated, these phases undergo reduction and release molecular oxygen. For example, under heating, hematite ($Fe^{+3}{}_2O_3$) is converted to magnetite ($Fe^{+2}Fe^{+3}{}_2O_4$), and pyrolusite ($Mn^{+4}O_2$) is converted to bixbyite ($Mn^{+3}{}_2O_3$). Further heating releases additional O_2, e.g., in the conversion of bixbyite to hausmannite ($Mn^{2+}Mn^{3+}{}_2O_4$). CheMin has detected hematite, akaganeite, goethite, and magnetite in Gale crater rocks, while ChemCam analyses suggest the presence of manganese oxides (Blake et al., 2013; Lanza et al., 2014; Rampe et al., 2017). The high abundance of X-ray amorphous material detected by CheMin is thought to partly consist of very fine grained mineral phases including nanophase Fe-oxide (Dehouck et al., 2014). The two key questions are whether these phases yield oxygen at appropriate temperatures, and whether there is adequate metal oxide in Gale crater rocks to account for the amount of oxygen observed by SAM.

Metal oxide equilibrium phase diagrams provide a starting point for characterizing the temperature of oxygen release from metal oxides. At thermodynamic equilibrium, the partial pressure of oxygen over a system containing both reduced and oxidized forms of a single metal is fixed and is a sensitive function of temperature and the given metal (e.g., Hasegawa, 2014). For example, the partial pressure of O_2 in equilibrium with coarsely crystalline MnO_2 and Mn_2O_3 at 200°C is 10^{-8} bar, increasing to 1 bar at 450°C (Birkner & Navrotsky, 2012). Therefore, as a metal oxide is heated, the O_2 partial pressure increases and the fraction of metal oxide in the more oxidized form decreases. Of interest due to the amorphous fraction observed by CheMin (Blake et al., 2013; Rampe et al., 2017), nanophase Mn- and Fe-oxides are less thermodynamically stable at a given temperature compared to their coarsely crystalline counterparts. For example, the equilibrium partial pressure of O_2 over nanophase MnO_2 at 200°C is ~10^{-5} bar, 1,000 times higher than over coarsely crystalline MnO_2 (Birkner & Navrotsky, 2012).

While thermodynamic considerations suggest oxygen release at SAM-relevant temperatures, an EGA run is not conducted at thermodynamic equilibrium. A He carrier gas is swept across the sample (Mahaffy et al., 2012), likely preventing the local oxygen partial pressure from ever achieving equilibrium with metal oxides present. Without kinetic limitations, continuous purging of evolved oxygen predicts O_2 generation at every

temperature throughout an EGA until the metal oxides are fully consumed. However, kinetic limitations almost certainly effect the rate of oxide decomposition. The temporal pattern of O_2 release from any metal oxides in an EGA must therefore be viewed as an intricate interplay of thermodynamics and kinetics. An O_2 peak (as opposed to continuous release) in an EGA could be generated as follows. At the start of the run, temperatures are so low that kinetic inhibition precludes substantial O_2 release. Because reaction rates typically scale exponentially with temperature, as the temperature rises in the run the O_2 release rate will increase rapidly. This creates the rising edge of the O_2 peak. With increasing temperature and associated oxygen release rate from the metal oxide in the EGA, the oxidized form of the metal oxide will approach exhaustion, the release rate will decline, and the O_2 peak height will fall. The temperature of maximum O_2 release in this scenario is controlled by kinetics and the amount of metal oxide present rather than directly by thermodynamics. We therefore consider the onset of O_2 release (a kinetic property of the metal oxide), rather than the peak of O_2 release (kinetics convolved with the amount present), to indicate the characteristic behavior of a metal oxide during EGA.

Previous work under SAM-like conditions indicates that MnO_2 releases O_2 at too high a temperature to be a candidate for the low-temperature O_2 release observed from Gale crater rocks (Hogancamp, Sutter, et al., 2018). We are not aware of any SAM-like experiments on hematite reduction in the literature.

To further inform the temperature of release of O_2 from iron and manganese oxides, especially nanophase materials (which favor lower temperature O_2 releases; Navrotsky et al., 2010), we undertook new EGA experiments under broadly SAM-like conditions. Experimental methods and detailed analytical results are provided in the supporting information. We analyzed Fe_2O_3 (600, 5, and 20 nm rod-like morphology grain sizes), MnO_2 (100 μm, 50 nm), and Mn_2O_3 (100, 30 nm). In all but two cases we analyzed a single pure metal oxide, with two runs of mixed phases to assess the possibility of back reaction of evolved O_2. Specifically, our goals were to assess the role of grain size on O_2 release temperature and establish whether these metal oxide phases evolve O_2 at temperatures compatible with the SAM releases attributed to perchlorate.

In the case of iron oxides, Figure 3 shows that the initiation of oxygen release from hematite occurs at >710°C for both 600 and 5 nm grain size. In contrast, the rod-shaped 20 nm hematite particles, specifically marketed as being "highly reactive," initiated oxygen release around 475°C. Although grain size/morphology clearly affects the temperature of O_2 release from hematite, these temperatures are still higher than the initiation of most of the SAM O_2 releases. These data preclude hematite as a candidate for the source of the SAM O_2. Similarly, because goethite and presumably akaganeite devolatilize to make hematite at low temperature (i.e., prior to metal reduction and O_2 release), and because magnetite is expected to release O_2 at even higher temperatures as it is more reduced than hematite, the common iron oxides all seem unlikely candidates.

Our results on manganese oxides are shown in Figure 3b (see Table S2 for detail). In the case of coarse (~100 μm) MnO_2, we found the initiation of O_2 release to occur at about 600°C, similar to the results obtained by Hogancamp, Sutter, et al. (2018) on a MnO_2 sample of unspecified grain size. However, we detected the onset of O_2 release from nanophase manganese oxides at much lower temperatures. In particular, both 50 nm MnO_2 particles and 100 nm Mn_2O_3 particles began to release oxygen at 350°C, while 30 nm Mn_2O_3 particles did so at ~310°C. That the less oxidized phase Mn_2O_3 began releasing oxygen at a temperature lower than the more oxidized MnO_2 is unexpected based on thermodynamics (Birkner & Navrotsky, 2012), suggesting that kinetics controlled by grain size is a major variable controlling the O_2 release temperature of Mn-oxides. The important role of grain size is reinforced by the slightly higher release temperature from 100 nm Mn_2O_3 compared to 30 nm Mn_2O_3.

Based solely on these analyses, nanophase Mn-oxides appear to be a feasible source of low-temperature oxygen release, with variations in onset temperature of release potentially attributable to variations in grain size. However, there are two observations that argue against such a role for manganese oxides. First, the Mn-oxides heated in this experiment released a second O_2 peak, beginning at 600–650°C. The relative amounts of O_2 released suggest that the second release is associated with reduction of Mn_3O_4 to MnO. The absence of a similar high-temperature O_2 release in the SAM data is evidence against Mn-oxides as the source of the O_2, unless that second release is back-reacted with the sample. For example, magnetite could plausibly be oxidized to hematite by the oxygen release associated with the conversion of Mn_3O_4 to MnO. To test this idea, two samples of MnO_2 were prepared: one intimately mixed with nanophase Fe_3O_4 as a weak reductant and

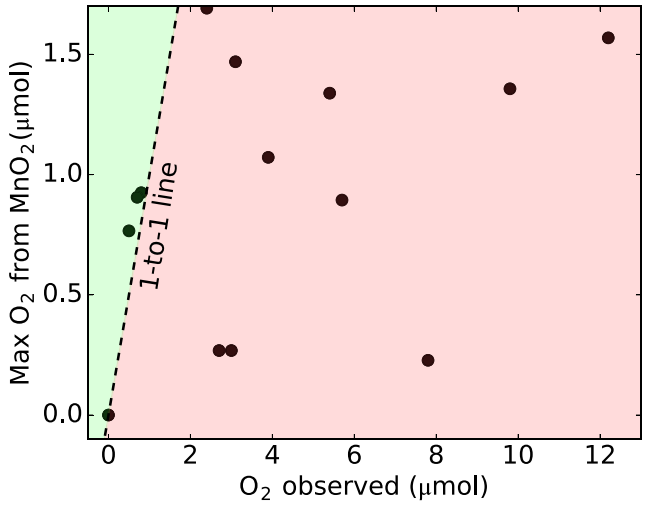

Figure 4. A comparison of the observed amount of O_2 released in each sample with the maximum amount possibly sourced from manganese, assuming that all Mn is present as MnO_2 and is reduced to MnO upon heating. Green shading indicates that O_2 can be accounted for assuming stoichiometric MnO_2; red shading indicates that O_2 cannot be accounted for with manganese.

one intimately mixed with nanophase Fe^0 as a strong reductant. No change in the O_2 release pattern was observed in the sample with admixed Fe_3O_4 compared to pure MnO_2. In contrast, the sample mixed with Fe^0 released no oxygen at all, illustrating that solid-gas reactions which consume O_2 are possible under SAM-like conditions. Further experiments on oxides of different composition and grain size could be undertaken to further investigate these reactions, but in the absence of compelling information on the actual properties of the Martian samples, such experiments are unlikely to definitively confirm or rule out their role in the SAM observations.

The second and stronger argument against nanophase Mn-oxides comes from mass balance. The presence of Mn-oxides in Gale crater rocks has been inferred by ChemCam via measurements of spatially discrete elevated Mn (Lanza et al., 2014, 2016), but it is not known whether all or any of the individual SAM samples include such elevated Mn. Here we develop the best-case assessment, in which all of the manganese in the APXS analyses of the SAM-analyzed samples is present in the form of manganese oxide. Manganese readily substitutes for iron in olivine, and since most of the olivine appears to have weathered away in Gale crater (Rampe et al., 2017), control of the manganese budget by Mn-oxides is a reasonable possibility. Which manganese oxidation state(s) are specifically present in Gale crater is not known, but a variety of poorly crystalline phases in an array of oxidation states tend to be intermingled in terrestrial occurrences of Mn-oxide (Post, 1999). Nevertheless, for present purposes we assume that all manganese is present in its most oxidized form, MnO_2. As shown in Figure 4, APXS-derived manganese concentrations do not correlate with the amount of O_2 released during EGA. More importantly, in most samples, the amount of O_2 released during SAM analysis is higher than can be associated with the amount of detected manganese, even if it is all present as MnO_2 (Figure 4). Unless the APXS measurements are in error by far more than their estimated 13% uncertainty (Campbell et al., 2012), or the O_2 measurements are systematically much higher than actual, this observation precludes Mn-oxides as the source of O_2 release in the SAM samples.

3.5. Perchlorate

Perchlorate demonstrates O_2 release at the temperatures observed in SAM, with the varied release temperatures ascribed to differing cation compositions (e.g., Leshin et al., 2013; Ming et al., 2014; Sutter et al., 2017). Adequate chlorine is present for the O_2 release to be entirely explained by the presence of perchlorate salts, assuming that a substantial but variable proportion of the chlorine is contained in perchlorate. Perchlorate has also been clearly detected on Mars at the Phoenix landing site (Hecht et al., 2009) and can account for the wide range of $\delta^{37}Cl$ compositions observed by SAM (Farley et al., 2016). These lines of evidence and the lack of evidence *against* perchlorate suggest that the presence of perchlorate in SAM samples is the most likely scenario to explain the O_2 release.

4. Modern Perchlorate

Although perchlorate offers the best explanation for oxygen release, indigenous ancient perchlorate is unlikely (section 2.1), indicating that any perchlorate observed in bedrock samples in Gale crater is probably young. An estimate of its maximum age can be obtained by extension of the radiolysis calculations presented for the Windjana sample in section 2.1.2. The perchlorate in this sample contains 14.4 ± 4.3% of the total chlorine. This proportion would be achieved after exposure to 38.0 ± 11.3 MGy of ionizing radiation assuming that all chlorine was originally perchlorate. Based on Windjana's estimated radioelement content, this dose would be reached in 2.4 ± 0.7 Ga. This constraint provides a firm upper limit to how long the perchlorate may have been present in the rock. In short, the perchlorate can only be Amazonian in age.

The presence of such youthful material in these ancient rocks requires explanation. Deliquescing perchlorate salts could form thin films of briny liquid which percolate into the bedrock through cracks and

fractures, depositing salts as they effloresce (Cull et al., 2010). As the Curiosity drill collects sample between 1.5 and 5 cm depth, the length scale of this percolation need only be on the order of a few centimeters. Such a process was inferred from the presence of a solubility-based gradient of sulfate salt coatings in the upper 15 cm of loose sediment exposed at the Troy site by the Spirit rover (Arvidson et al., 2010). Late-stage diagenetic vein-fill materials in Gale crater do not migrate outward (Nachon et al., 2014), suggesting that these rocks are impermeable. However, small-scale fracturing of the Gale crater bedrock could permit percolation of salts if such cracks formed after the fracture-fills. Freeze-thaw cycles are known to generate cracks at fractal scales (Lu et al., 2016), implying that the decameter-scale cracks observed in Gale crater (Oehler et al., 2016) may be an indication that such small-scale fracturing exists. Impacts are another likely source of rock fracture.

In this model, the variability of perchlorate concentration across the stratigraphic section could be explained by differing permeability associated with fracture abundance and/or secondary mineral formation. This model is purely conceptual, and further work is needed to explain the detailed variability in concentration between samples (e.g., why the presumably more permeable Windjana sandstone has far less perchlorate than the Cumberland mudstone sample and why multiple samples have no detectable perchlorate; Archer et al., 2019) and the reportedly varying cation chemistry of the perchlorate itself (Sutter et al., 2017). Potential mechanisms for modern perchlorate inclusion in ancient bedrock is an avenue of research that deserves further investigation.

5. Conclusions

The geologic history of Gale crater is not conducive to the deposition and preservation of indigenous perchlorate in the bedrock. The inferred abundance of perchlorate in several samples is too high for that perchlorate to have been present since deposition based on its rate of radiolytic destruction. Furthermore, the long-lived nature of the lacustrine succession and the lack of indicators of aridity such as bedded evaporites of less soluble salts, and associated sedimentary structures indicative of strongly evaporative processes, suggest that the deposition of highly soluble perchlorate salts as a native component of the Gale crater mudstones is unlikely.

The HCl and CH_3Cl in EGA initially thought to be related to perchlorate breakdown (Glavin et al., 2013; Ming et al., 2014) are shown here and elsewhere (Sutter et al., 2017) not to correlate with oxygen release. Therefore, there is no single direct line of evidence in SAM data that demands the presence of perchlorate in Gale crater. A large release of O_2 is the only observation attributed to perchlorate that cannot be explained via the presence of chloride salts. Regardless of the phase responsible, O_2 release upon heating is likely to destroy organic molecules by combustion (Lasne et al., 2016; ten Kate, 2010), making identification of the responsible chemical phase important in the search for biosignatures. We identify and assess five potential oxygen sources:

1. **Hydrogen peroxide/superoxides** are ruled out on the basis of the low temperatures (<200°C) at which they release oxygen.
2. **Trivalent (i.e., Fe- and Al-) sulfate salts** exhibit a generally high-temperature (>500°C) oxygen release which consistently correlates with SO_2 (Sutter et al., 2017), eliminating this possibility.
3. **Nitrate** releases both NO and O_2 in EGA, but the NO/O_2 ratio is too low (~1:20 as opposed to ~1:1) for the main source of O_2 to be nitrate.
4. **Mn-oxides,** especially at nanophase grain size, release oxygen at a temperature range consistent with the SAM data. However, a double-peaked release pattern and manganese mass balance present insurmountable challenges to this hypothesis. **Fe-oxides**, even at nanophase grain size, appear to release O_2 at too high a temperature.
5. **Perchlorate salts** have been shown to release oxygen at the temperatures observed by SAM (Sutter et al., 2017), and have been compellingly detected on Mars. Unusually ^{37}Cl-depleted and highly variable chlorine isotopes in Gale crater bedrock (Farley et al., 2016) support the presence of perchlorate on Mars by analogy to observed isotopes in the Atacama Desert on Earth.

Based on the radiolysis and geologic setting arguments, if perchlorate is indeed present, it is most likely geologically young (post mid-Amazonian). Given that the Phoenix mission landed in the Amazonian-age northern plains (Hecht et al., 2009) and all Martian meteorites containing perchlorate are Amazonian in age (Jaramillo et al., 2019; Kounaves et al., 2014), the only Martian materials suggested to contain ancient

perchlorate have been the drilled samples in Gale crater (Archer et al., 2016). If this proposed antiquity is conclusively eliminated, the only perchlorate observed on Mars would be geologically young. Without direct evidence for ancient perchlorate, whether perchlorate was present on early Mars or is exclusively an Amazonian phenomenon should be given further study. If early perchlorate is found to be unlikely, interpretations of data invoking perchlorate in an ancient (pre-Amazonian) setting would need to be evaluated for alternative explanations. We find geologically young perchlorate to be the most plausible explanation for the observation of O_2 release during EGA. A likely postdepositional source of perchlorate is percolation of thin films of briny liquid into rock pore space when sufficient humidity is present for deliquescence to occur. The exact mechanism of perchlorate inclusion deserves further detailed study.

Acknowledgments
We thank Brad Sutter for many thoughtful and spirited debates which improved this manuscript. We also thank the SAM and Curiosity teams for their support in rover operations, without which this work would not be possible. SAM data are available on the Planetary Data System (PDS; pds-geosciences.wustl.edu/missions/msl/sam.htm). Additional data used in this study are available on the CaltechDATA repository at https://doi.org/10.22002/D1.1299. Funding was provided by NASA.

References

Anderson, R. C., Jandura, L., Okon, A. B., Sunshine, D., Roumeliotis, C., Beegle, L. W., et al. (2012). Collecting samples in Gale Crater, Mars: An overview of the Mars Science Laboratory sample acquisition, sample processing and handling system. *Space Science Reviews*, *170*(1–4), 57–75. https://doi.org/10.1007/s11214-012-9898-9

Archer, P D, Ming, D. W., Sutter, B., Hogancamp, J. V., Morris, R., Clark, B. C., et al. (2019). Oxychlorine detection in Gale crater, Mars and implications for past environmental conditions, (2132) Presented at the 50th Lunar and Planetary Sciences Conference.

Archer, P. D, Ming, D. W., Sutter, B., Morris, R. V., Clark, B. C., Mahaffy, P. H., et al. (2016). Oxychlorine species on Mars: Implications from Gale crater samples. (2947). Presented at the 47th Lunar and Planetary Sciences Conference.

Archer, P. D., Franz, H. B., Sutter, B., Arevalo, R. D., Coll, P., Eigenbrode, J. L., et al. (2014). Abundances and implications of volatile-bearing species from evolved gas analysis of the Rocknest aeolian deposit, Gale crater, Mars. *Journal of Geophysical Research: Planets*, *119*, 237–254. https://doi.org/10.1002/2013JE004493

Arvidson, R. E., Bell, J. F., Bellutta, P., Cabrol, N. A., Catalano, J. G., Cohen, J., et al. (2010). Spirit Mars rover mission: Overview and selected results from the northern Home Plate Winter Haven to the side of Scamander crater. *Journal of Geophysical Research*, *115*, E00F03. https://doi.org/10.1029/2010JE003633

Atreya, S. K., & Gu, Z. G. (1994). Stability of the Martian atmosphere: Is heterogeneous catalysis essential? *Journal of Geophysical Research*, *99*(E6), 13,133–13,145. https://doi.org/10.1029/94JE01085

Atreya, S. K., Wong, A.-S., Renno, N. O., Farrell, W. M., Delory, G. T., Sentman, D. D., et al. (2006). Oxidant enhancement in Martian dust devils and storms: Implications for life and habitability. *Astrobiology*, *6*(3), 439–450. https://doi.org/10.1089/ast.2006.6.439

Biemann, K., & Bada, J. L. (2011). Comment on "Reanalysis of the Viking results suggests perchlorate and organics at midlatitudes on Mars" by Rafael Navarro-González et al. *Journal of Geophysical Research*, *116*, E12001. https://doi.org/10.1029/2011JE003869

Birkner, N., & Navrotsky, A. (2012). Thermodynamics of manganese oxides: Effects of particle size and hydration on oxidation-reduction equilibria among hausmannite, bixbyite, and pyrolusite. *American Mineralogist*, *97*(8–9), 1291–1298. https://doi.org/10.2138/am.2012.3982

Blake, D. F., Morris, R. V., Kocurek, G., Morrison, S., Downs, R. T., Bish, D., et al., & MSL Science Team (2013). Curiosity at Gale crater, Mars: Characterization and analysis of the Rocknest sand shadow. *Science*, *341*(6153), 1239505. https://doi.org/10.1126/science.1239505

Böhlke, J. K., Sturchio, N. C., Gu, B., Horita, J., Brown, G. M., Jackson, W. A., et al. (2005). Perchlorate isotope forensics. *Analytical Chemistry*, *77*(23), 7838–7842. https://doi.org/10.1021/ac051360d

Bristow, T. F., Rampe, E. B., Achilles, C. N., Blake, D. F., Chipera, S. J., Craig, P., et al. (2018). Clay mineral diversity and abundance in sedimentary rocks of Gale crater, Mars. *Science Advances*, *4*(6), eaar3330. https://doi.org/10.1126/sciadv.aar3330

Brown, G. M. (1986). The reduction of chlorate and perchlorate ions at an active titanium electrode. *Journal of Electroanalytical Chemistry and Interfacial Electrochemistry*, *198*(2), 319–330. https://doi.org/10.1016/0022-0728(86)90008-2

Brown, G. M., & Gu, B. (2006). The chemistry of perchlorate in the environment. In B. Gu, & J. D. Coates (Eds.), *Perchlorate: Environmental Occurrence, Interactions and Treatment*, (pp. 17–47). Boston, MA: Springer US. https://doi.org/10.1007/0-387-31113-0_2

Campbell, J. L., Perrett, G. M., Gellert, R., Andrushenko, S. M., Boyd, N. I., Maxwell, J. A., et al. (2012). Calibration of the Mars Science Laboratory Alpha Particle X-ray Spectrometer. *Space Science Reviews*, *170*(1-4), 319–340. https://doi.org/10.1007/s11214-012-9873-5

Cao, J., Elliott, D., & Zhang, W. (2005). Perchlorate reduction by nanoscale iron particles. *Journal of Nanoparticle Research*, *7*(4–5), 499–506. https://doi.org/10.1007/s11051-005-4412-x

Carrier, B. L., & Kounaves, S. P. (2015). The origins of perchlorate in the Martian soil. *Geophysical Research Letters*, *42*, 3739–3745. https://doi.org/10.1002/2015GL064290

Caswell, T. E., & Milliken, R. E. (2017). Evidence for hydraulic fracturing at Gale crater, Mars: Implications for burial depth of the Yellowknife Bay formation. *Earth and Planetary Science Letters*, *468*, 72–84. https://doi.org/10.1016/j.epsl.2017.03.033

Catling, D. C., Claire, M. W., Zahnle, K. J., Quinn, R. C., Clark, B. C., Hecht, M. H., & Kounaves, S. (2010). Atmospheric origins of perchlorate on Mars and in the Atacama. *Journal of Geophysical Research*, *115*, E00E11. https://doi.org/10.1029/2009JE003425

Chevrier, V. F., & Rivera-Valentin, E. G. (2012). Formation of recurring slope lineae by liquid brines on present-day Mars. *Geophysical Research Letters*, *39*, L21202. https://doi.org/10.1029/2012GL054119

Coates, J. D., & Achenbach, L. A. (2004). Microbial perchlorate reduction: Rocket-fuelled metabolism. *Nature Reviews Microbiology*, *2*(7), 569–580. https://doi.org/10.1038/nrmicro926

Cull, S. C., Arvidson, R. E., Catalano, J. G., Ming, D. W., Morris, R. V., Mellon, M. T., & Lemmon, M. (2010). Concentrated perchlorate at the Mars Phoenix landing site: Evidence for thin film liquid water on Mars. *Geophysical Research Letters*, *37*, L22203. https://doi.org/10.1029/2010GL045269

Dehouck, E., McLennan, S. M., Meslin, P., & Cousin, A. (2014). Constraints on abundance, composition, and nature of X-ray amorphous components of soils and rocks at Gale crater, Mars. *Journal of Geophysical Research: Planets*, *119*, 2640–2657. https://doi.org/10.1002/2014JE004716

Eggenkamp, H. (2014). Natural variations of stable chlorine and bromine isotopes on Earth. In *The Geochemistry of Stable Chlorine and Bromine Isotopes*, (pp. 115–144). Berlin, Heidelberg: Springer. https://doi.org/10.1007/978-3-642-28506-6_10

Eigenbrode, J. L., Summons, R. E., Steele, A., Freissinet, C., Millan, M., Navarro-González, R., et al. (2018). Organic matter preserved in 3-billion-year-old mudstones at Gale crater, Mars. *Science*, *360*(6393), 1096–1101. https://doi.org/10.1126/science.aas9185

Encrenaz, T., Bézard, B., Greathouse, T. K., Richter, M. J., Lacy, J. H., Atreya, S. K., et al. (2004). Hydrogen peroxide on Mars: Evidence for spatial and seasonal variations. *Icarus*, *170*(2), 424–429. https://doi.org/10.1016/j.icarus.2004.05.008

Ericksen, G. E. (1981). Geology and origin of the Chilean nitrate deposits (USGS Numbered Series No. 1188). U.S. G.P.O. : for sale by the Supt. of Docs., GPO,. Retrieved from http://pubs.er.usgs.gov/publication/pp1188

Farley, K., Malespin, C., Mahaffy, P., Grotzinger, J., Vasconcelos, P., Milliken, R., et al., & MSL Science Team (2014). In situ radiometric and exposure age dating of the Martian surface. *Science*, *343*(6169), 1247166. https://doi.org/10.1126/science.1247166

Farley, K. A., Martin, P., Archer, P. D. Jr., Atreya, S. K., Conrad, P. G., Eigenbrode, J. L., et al. (2016). Light and variable $^{37}Cl/^{35}Cl$ ratios in rocks from Gale Crater, Mars: Possible signature of perchlorate. *Earth and Planetary Science Letters*, *438*, 14–24. https://doi.org/10.1016/j.epsl.2015.12.013

Gallagher, P. K., Johnson, D. W., & Schrey, F. (1970). Thermal decomposition of iron (II) sulfates. *Journal of the American Ceramic Society*, *53*(12), 666–670. https://doi.org/10.1111/j.1151-2916.1970.tb12038.x

Gasnault, O., Mazoyer, J., Cousin, A., Meslin, P.-Y., Lasue, J., Lacour, J.-L., et al. (2012). Deciphering sample and atmospheric oxygen contents with ChemCam on Mars (2888). Presented at the 43rd Lunar and Planetary Science Conference.

Glavin, D. P., Freissinet, C., Miller, K. E., Eigenbrode, J. L., Brunner, A. E., Buch, A., et al. (2013). Evidence for perchlorates and the origin of chlorinated hydrocarbons detected by SAM at the Rocknest aeolian deposit in Gale crater. *Journal of Geophysical Research: Planets*, *118*, 1955–1973. https://doi.org/10.1002/jgre.20144

Gough, R. V., Chevrier, V. F., & Tolbert, M. A. (2014). Formation of aqueous solutions on Mars via deliquescence of chloride–perchlorate binary mixtures. *Earth and Planetary Science Letters*, *393*, 73–82. https://doi.org/10.1016/j.epsl.2014.02.002

Grotzinger, J. P., Gupta, S., Malin, M. C., Rubin, D. M., Schieber, J., Siebach, K., et al. (2015). Deposition, exhumation, and paleoclimate of an ancient lake deposit, Gale crater, Mars. *Science*, *350*(6257), aac7575. https://doi.org/10.1126/science.aac7575

Grotzinger, J. P., Sumner, D. Y., Kah, L., Stack, K., Gupta, S., Edgar, L., et al., & MSL Science Team (2014). A habitable fluvio-lacustrine environment at Yellowknife Bay, Gale crater, Mars. *Science*, *343*(6169), 1242777. https://doi.org/10.1126/science.1242777

Gu, B., Dong, W., Brown, G. M., & Cole, D. R. (2003). Complete degradation of perchlorate in ferric chloride and hydrochloric acid under controlled temperature and pressure. *Environmental Science & Technology*, *37*(10), 2291–2295. https://doi.org/10.1021/es0262378

Hardie, L., Smoot, J., & Eugster, O. (1978). *Lake sediments*. Hoboken, NJ: John Wiley & Sons.

Hasegawa, M. (2014). Chapter 3.3: Ellingham diagram. In S. Seetharaman (Ed.), *Treatise on Process Metallurgy*, (pp. 507–516). Boston: Elsevier. https://doi.org/10.1016/B978-0-08-096986-2.00032-1

Hecht, M. H., Kounaves, S. P., Quinn, R. C., West, S. J., Young, S. M. M., Ming, D. W., et al. (2009). Detection of perchlorate and the soluble chemistry of Martian soil at the Phoenix Lander site. *Science*, *325*(5936), 64–67. https://doi.org/10.1126/science.1172466

Hogancamp, J. V., Archer, P. D., Morris, R. V., Tu, V., Lanza, N., Sutter, B., et al. (2018). Detectability of manganese-bearing phases by the Sample Analysis at Mars (SAM) instrument on board the Curiosity rover in Gale crater, Mars (2482). Presented at the 49th Lunar and Planetary Science Conference.

Hogancamp, J. V., Sutter, B., Archer, D., Jr., Ming, D. W., & Mahaffy, P. R. (2017). Oxychlorine and chloride/ferrian saponite mixtures as a possible source of hydrochloric acid detected by the Sample Analysis at Mars (SAM) instrument in Gale crater, Mars. AGU Fall Meeting Abstracts, 51.

Hogancamp, J. V., Sutter, B., Morris, R. V., Archer, P. D., Ming, D. W., Rampe, E. B., et al. (2018). Chlorate/Fe-bearing phase mixtures as a possible source of oxygen and chlorine detected by the Sample Analysis at Mars instrument in Gale crater, Mars. *Journal of Geophysical Research: Planets*, *123*, 2920–2938. https://doi.org/10.1029/2018JE005691

Holt, B. D., & Engelkemeir, A. G. (1970). Thermal decomposition of barium sulfate to sulfur dioxide for mass spectrometric analysis. *Analytical Chemistry*, *42*(12), 1451–1453. https://doi.org/10.1021/ac60294a032

Jackson, W. A., Böhlke, J. K., Andraski, B. J., Fahlquist, L., Bexfield, L., Eckardt, F. D., et al. (2015). Global patterns and environmental controls of perchlorate and nitrate co-occurrence in arid and semi-arid environments. *Geochimica et Cosmochimica Acta*, *164*, 502–522. https://doi.org/10.1016/j.gca.2015.05.016

Jaramillo, E. A., Royle, S. H., Claire, M. W., Kounaves, S. P., & Sephton, M. A. (2019). Indigenous organic-oxidized fluid interactions in the Tissint Mars meteorite. *Geophysical Research Letters*, *46*, 3090–3098. https://doi.org/10.1029/2018GL081335

Keppler, F., Harper, D. B., Greule, M., Ott, U., Sattler, T., Schöler, H. F., & Hamilton, J. T. G. (2014). Chloromethane release from carbonaceous meteorite affords new insight into Mars lander findings. *Scientific Reports*, *4*(1), 1–11. https://doi.org/10.1038/srep07010

Kounaves, S. P., Carrier, B. L., O'Neil, G. D., Stroble, S. T., & Claire, M. W. (2014). Evidence of martian perchlorate, chlorate, and nitrate in Mars meteorite EETA79001: Implications for oxidants and organics. *Icarus*, *229*, 206–213. https://doi.org/10.1016/j.icarus.2013.11.012

Kounaves, S. P., Stroble, S. T., Anderson, R. M., Moore, Q., Catling, D. C., Douglas, S., et al. (2010). Discovery of natural perchlorate in the Antarctic dry valleys and its global implications. *Environmental Science & Technology*, *44*(7), 2360–2364. https://doi.org/10.1021/es9033606

Lanza, N. L., Fischer, W. W., Wiens, R. C., Grotzinger, J., Ollila, A. M., Cousin, A., et al. (2014). High manganese concentrations in rocks at Gale crater, Mars. *Geophysical Research Letters*, *41*, 5755–5763. https://doi.org/10.1002/2014GL060329

Lanza, N. L., Wiens, R. C., Arvidson, R. E., Clark, B. C., Fischer, W. W., Gellert, R., et al. (2016). Oxidation of manganese in an ancient aquifer, Kimberley formation, Gale crater, Mars. *Geophysical Research Letters*, *43*, 7398–7407. https://doi.org/10.1002/2016GL069109

Lasne, J., Noblet, A., Szopa, C., Navarro-González, R., Cabane, M., Poch, O., et al. (2016). Oxidants at the surface of Mars: A review in light of recent exploration results. *Astrobiology*, *16*(12), 977–996. https://doi.org/10.1089/ast.2016.1502

Le Deit, L., Hauber, E., Fueten, F., Mangold, N., Pondrelli, M., Rossi, A., & Jaumann, R. (2012). Model age of Gale crater and origin of its layered deposits. *LPI Contributions*, *1680*, 7045.

Leask, E. K., Ehlmann, B. L., Dundar, M. M., Murchie, S. L., & Seelos, F. P. (2018). Challenges in the search for perchlorate and other hydrated minerals with 2.1-μm absorptions on Mars. *Geophysical Research Letters*, *45*, 12,180–12,189. https://doi.org/10.1029/2018GL080077

Leshin, L. A., Mahaffy, P. R., Webster, C. R., Cabane, M., Coll, P., Conrad, P. G., et al. (2013). Volatile, isotope, and organic analysis of Martian fines with the Mars Curiosity rover. *Science*, *341*(6153), 1238937. https://doi.org/10.1126/science.1238937

Leshin, L. A., Mahaffy, P. R., Webster, C. R., Cabane, M., Coll, P., Conrad, P. G., et al. (2013). Volatile, isotope, and organic analysis of Martian fines with the Mars Curiosity rover. *Science*, *341*(6153), 1238937. https://doi.org/10.1126/science.1238937

Lu, Y., Liu, S., Weng, L., Wang, L., Li, Z., & Xu, L. (2016). Fractal analysis of cracking in a clayey soil under freeze–thaw cycles. *Engineering Geology*, *208*, 93–99. https://doi.org/10.1016/j.enggeo.2016.04.023

Mahaffy, P. R., Webster, C. R., Cabane, M., Conrad, P. G., Coll, P., Atreya, S. K., et al. (2012). The sample analysis at Mars investigation and instrument suite. *Space Science Reviews*, *170*(1–4), 401–478. https://doi.org/10.1007/s11214-012-9879-z

Marion, G. M., Catling, D. C., Zahnle, K. J., & Claire, M. W. (2010). Modeling aqueous perchlorate chemistries with applications to Mars. *Icarus*, *207*(2), 675–685. https://doi.org/10.1016/j.icarus.2009.12.003

Martin, P., Farley, K. A., Mahaffy, P. R., Malespin, C., & Vasconcelos, P. M. (2017). Landscape evolution mechanisms in Gale crater from in-situ measurement of cosmogenic noble gas isotopes. AGU Fall Meeting Abstracts, 52.

Martin, P. E., Farley, K. A., Baker, M. B., Malespin, C. A., Schwenzer, S. P., Cohen, B. A., et al. (2017). A two-step K-Ar experiment on Mars: Dating the diagenetic formation of jarosite from Amazonian groundwaters. *Journal of Geophysical Research: Planets*, *122*, 2803–2818. https://doi.org/10.1002/2017JE005445

McEwen, A. S., Ojha, L., Dundas, C. M., Mattson, S. S., Byrne, S., Wray, J. J., et al. (2011). Seasonal flows on warm Martian slopes. *Science*, *333*(6043), 740–743. https://doi.org/10.1126/science.1204816

McKay, C. P., Stoker, C. R., Glass, B. J., Davé, A. I., Davila, A. F., Heldmann, J. L., et al. (2013). The icebreaker life mission to Mars: A search for biomolecular evidence for life. *Astrobiology*, *13*(4), 334–353. https://doi.org/10.1089/ast.2012.0878

Ming, D. W., Archer, P. D., Glavin, D. P., Eigenbrode, J. L., Franz, H. B., Sutter, B., et al. (2014). Volatile and organic compositions of sedimentary rocks in Yellowknife Bay, Gale crater, Mars. *Science*, *343*(6169), 1245267. https://doi.org/10.1126/science.1245267

Mitra, K., & Catalano, J. G. (in press). Chlorate as a potential oxidant on Mars: Rates and products of dissolved Fe (II) oxidation, *Journal of Geophysical Research: Planets*. *124*(11), 2893–2916.https://doi.org/10.1029/2019JE006133

Morrison, S. M., Downs, R. T., Blake, D. F., Vaniman, D. T., Ming, D. W., Hazen, R. M., et al. (2018). Crystal chemistry of Martian minerals from Bradbury Landing through Naukluft Plateau, Gale crater, Mars. *American Mineralogist*, *103*(6), 857–871. https://doi.org/10.2138/am-2018-6124

Nachon, M., Clegg, S., Mangold, N., Schröder, S., Kah, L., Dromart, G., et al. (2014). Calcium sulfate veins characterized by ChemCam/Curiosity at Gale crater, Mars. *Journal of Geophysical Research: Planets*, *119*, 1991–2016. https://doi.org/10.1002/2013JE004588

Navarro-González, R., Vargas, E., de la Rosa, J., Raga, A. C., & McKay, C. P. (2010). Reanalysis of the Viking results suggests perchlorate and organics at midlatitudes on Mars. *Journal of Geophysical Research*, *115*, E12010. https://doi.org/10.1029/2010JE003599

Navrotsky, A., Ma, C., Lilova, K., & Birkner, N. (2010). Nanophase transition metal oxides show large thermodynamically driven shifts in oxidation-reduction equilibria. *Science*, *330*(6001), 199–201. https://doi.org/10.1126/science.1195875

Oehler, D. Z., Mangold, N., Hallet, B., Fairén, A. G., Deit, L. L., Williams, A. J., et al. (2016). Origin and significance of decameter-scale polygons in the lower Peace Vallis fan of Gale crater, Mars. *Icarus*, *277*, 56–72. https://doi.org/10.1016/j.icarus.2016.04.038

Ojha, L., Wilhelm, M. B., Murchie, S. L., McEwen, A. S., Wray, J. J., Hanley, J., et al. (2015). Spectral evidence for hydrated salts in recurring slope lineae on Mars. *Nature Geoscience*, *8*(11), 829–832. https://doi.org/10.1038/ngeo2546

Oren, A., Elevi Bardavid, R., & Mana, L. (2014). Perchlorate and halophilic prokaryotes: Implications for possible halophilic life on Mars. *Extremophiles*, *18*(1), 75–80. https://doi.org/10.1007/s00792-013-0594-9

Orosei, R., Lauro, S. E., Pettinelli, E., Cicchetti, A., Coradini, M., Cosciotti, B., et al. (2018). Radar evidence of subglacial liquid water on Mars. *Science*, *361*(6401), 490–493. https://doi.org/10.1126/science.aar7268

Oyama, V. I., & Berdahl, B. J. (1977). The Viking Gas Exchange Experiment results from Chryse and Utopia surface samples. *Journal of Geophysical Research*, *82*(28), 4669–4676. https://doi.org/10.1029/JS082i028p04669

Pavlov, A. A., Vasilyev, G., Ostryakov, V. M., Pavlov, A. K., & Mahaffy, P. (2012). Degradation of the organic molecules in the shallow subsurface of Mars due to irradiation by cosmic rays. *Geophysical Research Letters*, *39*, L13202. https://doi.org/10.1029/2012GL052166

Post, J. E. (1999). Manganese oxide minerals: Crystal structures and economic and environmental significance. *Proceedings of the National Academy of Sciences*, *96*(7), 3447–3454. https://doi.org/10.1073/pnas.96.7.3447

Prince, L. A., & Johnson, E. R. (1965a). The radiation-induced decomposition of the alkali and alkaline Earth perchlorates. I. Product yields and stoichiometry[1a]. *The Journal of Physical Chemistry*, *69*(2), 359–377. https://doi.org/10.1021/j100886a002

Prince, L. A., & Johnson, E. R. (1965b). The radiation-induced decomposition of the alkali and alkaline Earth perchlorates. II. Mechanism of the decomposition[1a]. *The Journal of Physical Chemistry*, *69*(2), 377–384. https://doi.org/10.1021/j100886a003

Quinn, R. C., Martucci, H. F. H., Miller, S. R., Bryson, C. E., Grunthaner, F. J., & Grunthaner, P. J. (2013). Perchlorate radiolysis on Mars and the origin of Martian soil reactivity. *Astrobiology*, *13*(6), 515–520. https://doi.org/10.1089/ast.2013.0999

Rampe, E. B., Ming, D. W., Blake, D. F., Bristow, T. F., Chipera, S. J., Grotzinger, J. P., et al. (2017). Mineralogy of an ancient lacustrine mudstone succession from the Murray formation, Gale crater, Mars. *Earth and Planetary Science Letters*, *471*, 172–185. https://doi.org/10.1016/j.epsl.2017.04.021

Smith, M. L., Claire, M. W., Catling, D. C., & Zahnle, K. J. (2014). The formation of sulfate, nitrate and perchlorate salts in the Martian atmosphere. *Icarus*, *231*, 51–64. https://doi.org/10.1016/j.icarus.2013.11.031

Srinivasan, R., Sorial, G., & Sahle-Demessie, E. (2009). Removal of perchlorate and chlorate in aquatic systems using integrated technologies. *Environmental Engineering Science*, *26*(11), 1661–1671. https://doi.org/10.1089/ees.2009.0153

Stack, K. M., Grotzinger, J. P., Lamb, M. P., Gupta, S., Rubin, D. M., Kah, L. C., et al. (2019). Evidence for plunging river plume deposits in the Pahrump Hills member of the Murray formation, Gale crater, Mars. *Sedimentology*, *66*(5), 1768–1802. https://doi.org/10.1111/sed.12558

Steele, A., Benning, L. G., Wirth, R., Siljeström, S., Fries, M. D., Hauri, E., et al. (2018). Organic synthesis on Mars by electrochemical reduction of CO2. *Science Advances*, *4*(10), eaat5118. https://doi.org/10.1126/sciadv.aat5118

Stein, N., Grotzinger, J. P., Schieber, J., Mangold, N., Hallet, B., Newsom, H., et al. (2018). Desiccation cracks provide evidence of lake drying on Mars, Sutton Island member, Murray formation, Gale Crater. *Geology*, *46*(6), 515–518. https://doi.org/10.1130/G40005.1

Stern, J. C., Sutter, B., Freissinet, C., Navarro-González, R., McKay, C. P., Archer, P. D. Jr., et al., & the MSL Science Team (2015). Evidence for indigenous nitrogen in sedimentary and aeolian deposits from the Curiosity rover investigations at Gale crater, Mars. *Proceedings of the National Academy of Sciences*, *112*(14), 4245–4250. https://doi.org/10.1073/pnas.1420932112

Stern, J. C., Sutter, B., Jackson, W. A., Navarro-González, R., McKay, C. P., Ming, D. W., et al. (2017). The nitrate/(per)chlorate relationship on Mars. *Geophysical Research Letters*, *44*, 2643–2651. https://doi.org/10.1002/2016GL072199

Sutter, B., McAdam, A. C., Mahaffy, P. R., Ming, D. W., Edgett, K. S., Rampe, E. B., et al. (2017). Evolved gas analyses of sedimentary rocks and eolian sediment in Gale crater, Mars: Results of the Curiosity rover's sample analysis at Mars instrument from Yellowknife Bay to the Namib Dune. *Journal of Geophysical Research: Planets*, *122*, 2574–2609. https://doi.org/10.1002/2016JE005225

Taylor, G. J. (2013). The bulk composition of Mars. *Geochemistry*, *73*(4), 401–420. https://doi.org/10.1016/j.chemer.2013.09.006

Taylor, G. J., Stopar, J. D., Boynton, W. V., Karunatillake, S., Keller, J. M., Brückner, J., et al. (2007). Variations in K/Th on Mars. *Journal of Geophysical Research*, *112*, E03S06. https://doi.org/10.1029/2006JE002676

Taylor, S. R., & McLennan, S. (2009). *Planetary crusts: Their composition, origin and evolution*. Cambridge: Cambridge University Press.

ten Kate, I. L. (2010). Organics on Mars? *Astrobiology*, *10*(6), 589–603. https://doi.org/10.1089/ast.2010.0498

Thomas, N. H., Ehlmann, B. L., Meslin, P.-Y., Cousin, A., Forni, O., Rapin, W., et al. (2018). MSL ChemCam observations of chloride salts in Gale crater, Mars (2876). Presented at the 49th Lunar and Planetary Science Conference.

Toner, J. D., Catling, D. C., & Light, B. (2014). The formation of supercooled brines, viscous liquids, and low-temperature perchlorate glasses in aqueous solutions relevant to Mars. *Icarus*, *233*, 36–47. https://doi.org/10.1016/j.icarus.2014.01.018

Toner, J. D., Catling, D. C., & Light, B. (2015). A revised Pitzer model for low-temperature soluble salt assemblages at the Phoenix site, Mars. *Geochimica et Cosmochimica Acta*, *166*, 327–343. https://doi.org/10.1016/j.gca.2015.06.011

Tosca, N. J., McLennan, S. M., Clark, B. C., Grotzinger, J. P., Hurowitz, J. A., Knoll, A. H., et al. (2005). Geochemical modeling of evaporation processes on Mars: Insight from the sedimentary record at Meridiani Planum. *Earth and Planetary Science Letters*, *240*(1), 122–148. https://doi.org/10.1016/j.epsl.2005.09.042

Turner, A. M., Abplanalp, M. J., & Kaiser, R. I. (2016). Mechanistic studies on the radiolytic decomposition of perchlorates on the Martian surface. *The Astrophysical Journal*, *820*(2), 127. https://doi.org/10.3847/0004-637X/820/2/127

Urbansky, E. T. (2002). Perchlorate as an environmental contaminant. *Environmental Science and Pollution Research*, *9*(3), 187–192. https://doi.org/10.1007/BF02987487

Van Schmus, W. R. (1995). Natural radioactivity of the crust and mantle. In *Global Earth Physics*, (pp. 283–291). Washington, DC: American Geophysical Union (AGU). https://doi.org/10.1029/RF001p0283

Vaniman, D., Bish, D., Ming, D., Bristow, T., Morris, R., Blake, D., et al., & MSL Science Team (2014). Mineralogy of a mudstone at Yellowknife Bay, Gale crater, Mars. *Science*, *343*(6169), 1243480. https://doi.org/10.1126/science.1243480

Vaniman, D. T., Martínez, G. M., Rampe, E. B., Bristow, T. F., Blake, D. F., Yen, A. S., et al. (2018). Gypsum, bassanite, and anhydrite at Gale crater, Mars. *American Mineralogist*, *103*(7), 1011–1020. https://doi.org/10.2138/am-2018-6346

Vasconcelos, P., Farley, K., Malespin, C., Mahaffy, P., Ming, D., McLennan, S., et al. (2016). Discordant K-Ar and young exposure dates for the Windjana sandstone, Kimberley, Gale crater, Mars. *Journal of Geophysical Research: Planets*, *121*, 2176–2192. https://doi.org/10.1002/2016JE005017

Wänke, H., Dreibus, G., Wright, I. P., Herbert, C. S. W., Keith, R. S., & Southwood, D. J. (1994). Chemistry and accretion history of Mars. *Philosophical Transactions of the Royal Society of London. Series A: Physical and Engineering Sciences*, *349*(1690), 285–293. https://doi.org/10.1098/rsta.1994.0132

Wilson, E. H., Atreya, S. K., Kaiser, R. I., & Mahaffy, P. R. (2016). Perchlorate formation on Mars through surface radiolysis-initiated atmospheric chemistry: A potential mechanism. *Journal of Geophysical Research: Planets*, *121*, 1472–1487. https://doi.org/10.1002/2016JE005078

Yen, A. S., Kim, S. S., Hecht, M. H., Frant, M. S., & Murray, B. (2000). Evidence that the reactivity of the Martian soil is due to superoxide ions. *Science*, *289*(5486), 1909–1912. https://doi.org/10.1126/science.289.5486.1909

Zent, A. P., Ichimura, A. S., Quinn, R. C., & Harding, H. K. (2008). The formation and stability of the superoxide radical (O_2^-) on rock-forming minerals: Band gaps, hydroxylation state, and implications for Mars oxidant chemistry. *Journal of Geophysical Research*, *113*, E09001. https://doi.org/10.1029/2007JE003001

Zhao, Y.-Y. S., McLennan, S. M., Jackson, W. A., & Karunatillake, S. (2018). Photochemical controls on chlorine and bromine geochemistry at the Martian surface. *Earth and Planetary Science Letters*, *497*, 102–112. https://doi.org/10.1016/j.epsl.2018.06.015

References From the Supporting Information

Farley, K. A., Reiners, P. W., & Nenow, V. (1999). An apparatus for high-precision helium diffusion measurements from minerals. *Analytical Chemistry*, *71*(10), 2059–2061. https://doi.org/10.1021/ac9813078

Till, J. L., Guyodo, Y., Lagroix, F., Morin, G., & Ona-Nguema, G. (2015). Goethite as a potential source of magnetic nanoparticles in sediments. *Geology*, *43*(1), 75–78. https://doi.org/10.1130/G36186.1